Anonymous Referee #2:

We would like to thank the referee for the valuable comments. Listed below are our responses to the comments and the corresponding changes made to the revised manuscript. The comments of the referee are marked in black and the answers are marked in blue.

1. Summary

The article by Zhang et al. retreads a lot of information already covered in Zhang et al. (AMT, 2016), with some additional analysis. Overall, I find there are potentially some interesting components of this paper that go beyond the author's previous work, but at the same time there are a number of aspects that are presented as novel insights that are either not sufficiently justified or explained, or are simply wrong. I cannot recommend this paper for publication. The authors should work to truly distinguish it from their previous work. My specific comments follow below (in chronological order, mainly).

Response: We thank the reviewer for raising this question and we hope that the reviewer will be convinced after our detailed clarification below.

Although based on the same data sets as in the current manuscript, the previous paper "Measuring the morphology and density of internally mixed black carbon with SP2 and VTDMA " by Zhang et al. (AMT, 2016) specifically focused on:

- demonstrated an technical approach to determine the effective density of black carbon (BC) cores for internally-mixed BC particles by a combined system of Single Particle Soot Photometer (SP2) and Volatility Tandem Differential Mobility Analyzer (VTDMA).

In the current study, we

- presented the general feature of the BC mixing state: size distribution, number/mass fraction, diurnal variation, turnover rate, and coating thickness at a polluted sub-urban area of Beijing, China, in summer time;
- validated the sizing ability of SP2 (from ~200 nm to 400 nm) and further explored the possibility of using LEO-fit method to extend its sizing ability towards larger size range (i.e., from ~400 nm up to ~550 nm, usually the SP2 scattering signal becomes saturated with particles larger than 400 nm);
- compared the size distribution of BC-cores from SP2 with that of non-volatile cores from VTDMA, revealing a large fraction of low volatile non-BC components.

The above major results have not been included in the AMT paper, and we feel that the two papers are readily distinguishable. It would be helpful if the reviewer could kindly specify the content that he/she considered as republishing, we may then further clarify it in more details.

2. Specific comments

(1) Consideration of the PSL's in Fig. 2 demonstrates that the observation of a wide band of refractive index values is a result of variability in particles passing through the SP2 laser and is not due to the distribution of diameters coming out of the DMA. This information can be translated into an effective uncertainty in the size of a given particle. Using the central RI value, a distribution of sizes can be constructed that would also reproduce the observed scatter. This should be considered. Very approximately, +/- 0.1 in RI space = +/- 20 nm in diameter space.

Response: Thanks to the reviewer for raising this concern. We, however, do not think that Fig. 2 is a result of variability in the particle passing through the laser. (1) The SP2 that we used in the field has been properly optically aligned and calibrated. The laser focus has been checked with beam-scan camera and showed one nice Gaussian

distribution. (2) The diameter of PSL standard particles is usually centered at certain diameter with a distribution. Here we performed additional lab experiments to measure the number size distribution of the generated PSL standard particles (203 nm) with a Scanning Mobility Particle Sizer (SMPS, TSI 3936) and SP2. Figure R1 shows very similar normalized number size distribution of 203 nm PSL standard particles measured by SMPS (black curve) and SP2 (red curve). Thus, the distribution of PSL particles measured by SP2 in Figure 2 is not a result of variability in particles passing through the SP2 laser but rather the nature of the PSL standard particles, which corresponding to a span of refractive index of ~1.4 (~230 nm) to 1.8 (~180 nm) if all PSL particles are assumed to be 203 nm.
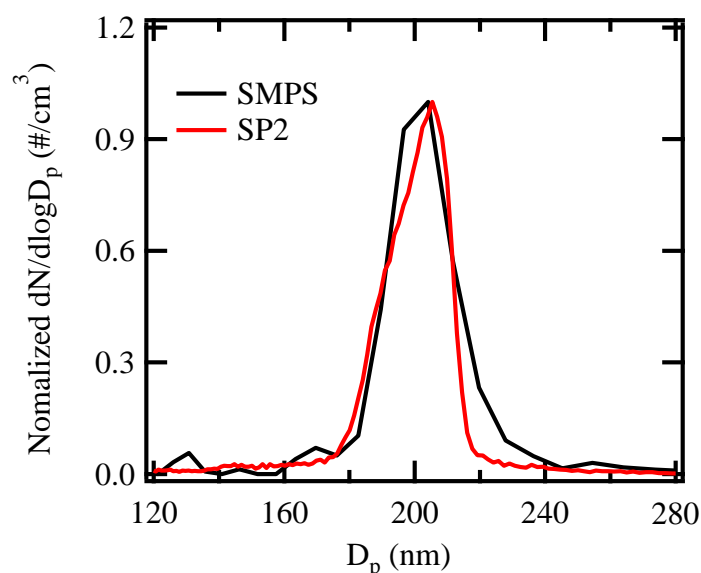
Fig. R1. The size distribution of PBL at 203 nm using SMPS and SP2 measurements.

(2) Page 5: I have no idea what "bones and flesh" means. This is not at all common scientific language, nor is it clear in the usage.

Response: Thanks for the comment and the metaphor that we are using here may not be appropriate. We hope the revised description "the voids among carbon spherules filled by non-BC components" is clearer to the reviewer.

(3) Eqn. 6: It is unclear where this equation comes from. It appears to be made up by the authors. Does the use of this equation have a justification? I don't see how this is physically justifiable.

Response: Thanks. This equation has been widely used in previous studies (e.g., Hänel, et al. 1968; Marley et al., 2001; Bond and Bergstrom, 2006; Schkolnik et al., 2007) to calculate the volume averaged refractive index. That is, the refractive index of a mixture particle can be calculated as the volume weighted average of the refractive indices of all components, as $\tilde{m} = \sum_i \tilde{m}_i c_i$, where $\tilde{m}$ is the refractive index of a mixture particle; $\tilde{m}_i$ is the refractive index of particle species; c is the volume ratio of particle species;. For example, Schkolnik et al. (2007) calculated the refractive index of biomass burning aerosol as the volume average of the refractive indices of elemental and organic carbon. Also, Bond and Bergstrom (2006) determined the refractive index of fresh BC as the volume average of the refractive indices of void-free carbon (1.95–0.79i at 550 nm) and air (1.00–0.00i).

In our study, assuming spherical morphology of the internally mixed BC particles, the void ratio R_{void} is the volume fraction of void. According to the above equation, the refractive index of the particles therefore can be calculated as Eq. (6).

To make this point clear, we will be revised the description of Eq. (6) in the manuscript after having the comments from all the reviewers.

(4) I understand the idea of adjusting the RI for non-BC containing particles to match with the selected mobility diameter, as it is not unreasonable to think that the non-BC containing particles are spherical. However, I do not understand the justification for this for BC-containing ("internally mixed") particles that are not necessarily spherical and for which the extent of sphericity is likely linked to the amount of coating material. The relationship between mobility diameter and actual particle size (characterized in some particular manner) will be dependent upon the particle shape. Thus, it is not clear how, for internally mixed particles, the tuning which the authors have done actually leads to an improvement in the estimated size. They have imparted some assumption regarding shape that has not been justified.

Response: Thanks for the comments. There might be some misunderstanding on the data process and analyzing procedure and we would like to kindly clarify that the optical calculations for non-BC and internally-mixed BC particles are different in our study. Here, we make a chart (Figure R2) to illustrate the whole data process and analyzing procedure. For non-BC particles, we matched the optical diameter to the electro-mobility diameter by tuning its refractive index (RI), marked red in Figure R2. The retrieved RI for non-BC particles (~1.42 - 0i) seems to be independent on particle size (Figure 2 in the manuscript). But, for the internally-mixed BC containing particles, when retrieving its optical diameter with the LEO-fit method (Gao et al. 2007), we did not adjust RI for either BC core or coating materials. In the LEO-fit calculation, RI for coating material was assumed to be same as the RI of non-BC particles (fixed with ~1.42 - 0i). RI for BC core was estimated as the volume weighted average of the RI of void and BC as Eq. 6 in the manuscript, marked green in Figure R2. Diameter of BC core was calculated from the BC mass given by SP2 and the predefined BC effective density (1.2 g/cm^3), marked yellow in Figure R2. The volume of void in the BC core and the BC core effective density are determined by the method introduced in Zhang et al. (AMT, 2016). After getting the diameter and RI of BC core, RI of coating material and the scattering signal of BC-containing particles from SP2, we used LEO-fit combined with Mie model to retrieved the optical diameter of BC-contain particles (marked blue in Fig. R2), following the LEO-fit method introduced by Gao et al. (2007).
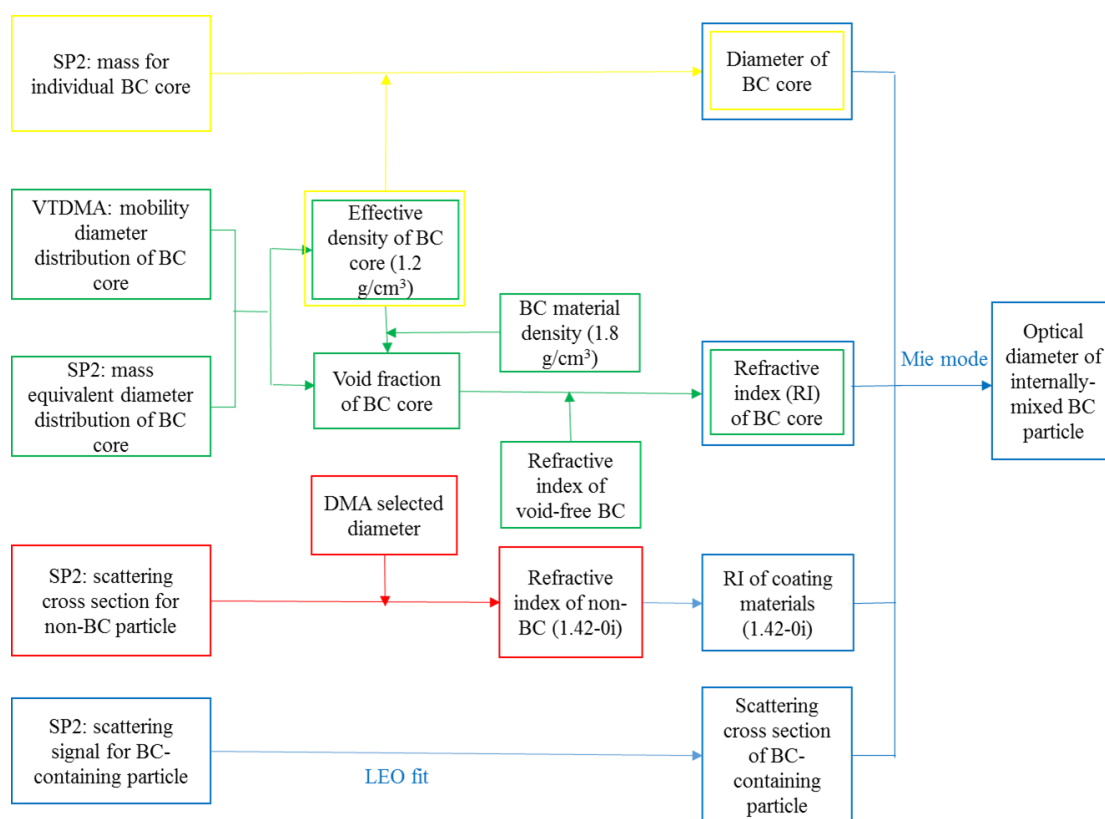
Fig. R2 (Figure. S2 in the revised manuscript). Schematic of optical size calculation for internally-mixed BC particle.

In the Mie calculation, spherical shape was assumed for internally mixed BC particles. We agree with the reviewer that the BC-containing particles are not necessarily spherical. However, as can be seen in Fig. 3b, the optical diameter of the internally-mixed BC particles derived with the LEO-fit method agrees very well with their mobility diameter, which implies that the internally-mixed BC containing particles are very likely in a spherical or near-spherical shape at Xianghe site, which may due to the strong chemical aging in the polluted atmosphere around Beijing in North China Plain.

To make this point clear, we have revised the Sect. 2.2.3 in the manuscript: "The optical size of non-BC and internally-mixed BC particles derived from SP2 was retrieved using LEO fit and Mie calculation. The whole data process and analyzing procedure are illustrated in Fig. S2.

For non-BC particle, its optical diameter $D_{opt,non-BC}$ can be determined from its

scattering cross section (C_s) and the refractive index (RI_{non-BC}) of non-BC components (Cheng et al., 2009; Cheng et al., 2006), as Eq. (3):

$$D_{opt,non-BC} \sim (C_s, \ RI_{non-BC}), \qquad (3)$$

In this study, C_s was determined by the LEO fit of SP2 scattering signal (Gao et al., 2007). RI_{non-BC} was determined through a closure study: we matched the optical diameter to the electro-mobility diameter by tuning its refractive index (RI), marked red in Fig. S2. The retrieved RI for non-BC particles (~1.42 - 0i) seems to be independent on particle size. For the validation, we also applied this method to polystyrene latex (PSL) spheres. As shown in Fig. 2, the inversion gives a peak RI of 1.5861, the same as the RI of PSL (1.59) in literature (Gao et al., 2007).

For internally-mixed BC particle, its optical size is related to its scattering cross section (C_s), the diameter of the BC core (D_c) and the refractive index of BC core (RI_c) and coating material (RI_{cm}) (Cheng et al., 2009; Cheng et al., 2006), as Eq. (4):

$$D_{opt,In-BC} \sim (C_s, D_c, RI_{cm}, RI_c) \sim (C_s, M, \rho_{eff}, RI_{cm}, RI_c), \qquad (4)$$

In Eq. (4), RI_{cm} is equal to RI_{non-BC} (1.42 - 0i), assuming that coating materials on BC surface have the same components with non-BC particles. D_c was calculated from the BC mass given by SP2 and the predefined BC effective density (1.2 g/cm^3, Zhang et al. 2016b) as Eq. (5), marked yellow in Fig. S2.

$$D_c = (\frac{6m}{\pi \rho_{eff}})^{\frac{1}{3}}, \qquad (5)$$

For RI_c in Eq. (4), we assume that BC and some non-BC materials together make a spherical core and the voids among carbon spherules filled by non-BC components. Then RI_c in was estimated as the volume weighted average of the RI of void and BC as Eq. (6), marked green in Fig. S2:

$$RI_c = [n_{BC} \times (1 - R_{void}) + n_{nonBC} \times R_{void}] + [k_{BC} \times (1 - R_{void})]i, \qquad (6)$$

in which, n_{BC} and n_{nonBC} are the real parts of RI for the BC materials and non-BC components (n_{BC} = 1.95 and n_{nonBC} = 1.42); k_{BC} is the imaginary part of the refractive index for BC (k_{BC} = 0.79) (Bond and Bergstrom, 2006); R_{void} (~0.30) is determined by the method introduced in Zhang et al. (AMT, 2016).

After getting the diameter and RI of BC core, RI of coating material and the

scattering signal of internally-mixed BC particles from SP2, we used LEO-fit combined with Mie model to retrieved the optical diameter of internally-mixed BC particles (marked blue in Fig. S2), following the LEO-fit method introduced by Gao et al. (2007)."

(5) I do not find Fig. 3 useful. It would only be surprising if the agreement between the "optical" and "prescribed" diameters was bad, given that they have tuned the RI to make the two match. All the authors are showing is that their tuning has worked to make the Doptical match the Dmobility. Also, this is not a validation of the "assumption of spherical BC particle[sic] in the Mie model calculation." The authors have forced agreement, not demonstrated anything about sphericity. Their method says little about the method "accuracy" (P6, L16)?

Response: As explained in our response to comment 4, for internally-mixed BC particles, we did not tune RI to force the agreement. RI for the coating materials was assumed to be same as that of non-BC containing particles, and RI for BC core was estimated as Eq. 6 in the manuscript. Therefore, the good agreement between the optical diameter derived from the LEO-fit method and the particle mobility diameter selected by the DMA implies that the internally-mixed BC containing particles are very likely in a spherical or near-spherical shape at Xianghe site, which may due to the strong chemical aging in the polluted atmosphere around Beijing in North China Plain. To this end, we would like to keep Fig. 3B in the manuscript (Figure R3B in this response).

The comparison of optical sizing from 400 nm to ~550 nm in Fig. 3A (Figure R3A in this response) can be taken as a validation of the LEO-fit method. For non-BC containing particles larger than 400 nm, the scattering signal in SP2 would have been saturated. That is why the 400 nm was usually taken as the upper sizing limit of SP2. The optical diameters of the large non-BC containing particles (from ~400 nm up to ~550 nm) were retrieved by LEO-fit method (Gao, et al., 2007). In Fig 3A (Figure R3A in this response), we can see that for those large particles (from ~400 nm up to

~550 nm) the retrieved optical diameters fit well with their mobility diameters. Therefore, we further demonstrate in that the optical diameters of the large particles (from ~400 nm up to ~550 nm) can be still retrieved from the LEO-fit method (Gao, et al., 2007). Therefore, we would like to keep Fig. 3A (Figure R3A in this response) in the manuscript.

To make the purpose of plot clearer, we mark the signal saturation point (~400 nm) as green dashed line in Figure 3. We have revised the discussion on Fig. 3 in the manuscript: "Figure 3 compares the optical diameter (determined by the SP2) for non-BC and internally-mixed BC particles with the mobility diameter (determined by the DMA1). The combination of DMA with SP2 makes it possible to distinguish singly charged particles from the doubly/multiply charged particles. Here, we compared the optical diameter of doubly/multiply charged particles with the nominal mobility sizes of those particles (red circles in Fig. 3). The optical particle diameter showed an excellent agreement with the mobility diameter, with an average difference of ~1%.

For non-BC particles, the agreement of optical sizing from 400 nm to ~550 nm with mobility size in Fig. 3A demonstrated the validation of the LEO-fit method. For non-BC containing particles larger than 400 nm, the scattering signal in SP2 would have been saturated. That is why the 400 nm was usually taken as the upper sizing limit of SP2. The optical diameters of the large non-BC containing particles (from ~400 nm up to ~550 nm) were retrieved by LEO-fit method (Gao, et al., 2007). In Fig 3A, we can see that for those large particles (from ~400 nm up to ~550 nm) the retrieved optical diameters fit well with their mobility diameters. Therefore, we further demonstrate in that the optical diameters of the large particles (from ~400 nm up to ~550 nm) can be still retrieved from the LEO-fit method.

For internally-mixed BC particles, the good agreement between the optical diameter derived from the LEO-fit method and the particle mobility diameter selected by the DMA in Fig. 3B implies that the internally-mixed BC containing particles are very likely in a spherical or near-spherical shape at Xianghe site, which may due to

the strong chemical aging in the polluted atmosphere around Beijing in North China Plain. Therefore, the assumption on a spherical particle for internally mixed BC in the Mie model calculation should be valid in our case."
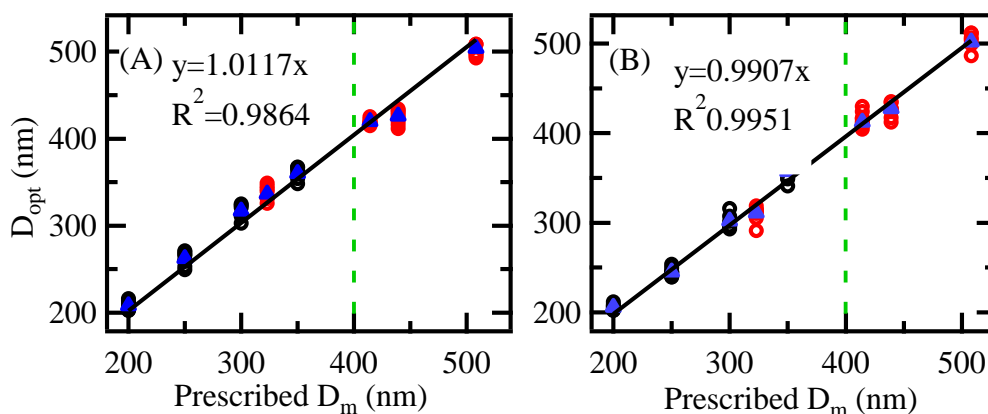
Fig. R3. (Figure 3 in the revised manuscript) Comparison of the prescribed mobility size (D_m) by DMA1 and the optical size (D_{opt}) determined by SP2 for (A) non-BC particles and (B) internally-mixed BC particles. The solid lines are fitted based on average data (blue triangle); the black circles and red circles represent the singly charged particle samples and doubly/ multiply charged particle samples, respectively. Particles those are larger than 400 nm (marked as green dash line) will usually saturate the scattering detection channel of SP2.

6) I find the authors' terminology regarding "non-BC", "internally-mixed BC" and "externally-mixed BC" confusing. There are non-BC and BC-containing particles. For BC-containing particles, there is then a distribution of relative coating amounts, with some particles having little coating (which I think the authors take to mean "externally mixed") and some having a lot of coating (here, I think, "internally mixed"). The authors make their definition based on a "lag-time" analysis. But, the validity of such a binary framework has not been justified here. Do they find a bimodal distribution of lagtimes, thus justifying the binary framework?

Response: Thanks and yes, we did find a bimodal distribution of lag-times (Fig. R4). Here we adopted a classification method based on a threshold lag-time/coating thickness) which is commonly used previous studies (e.g., Schwarz et al., 2006; Sedlacek et al., 2012; Subramanian et al., 2010). In literature, the two peaks were always observed and considered as the externally-mixed BC and internally-mixed BC, respectively.

We include the Figure R4 about the distribution of lag-time in our SP2 measurements as Figure S1 in supplementary information. We will clarify the terminology about 'non-BC particles', 'BC-containing particles' and the sub categories of 'externally mixed BC (very thin coating)' and 'internally-mixed BC (thick coating)' in the revised manuscript.
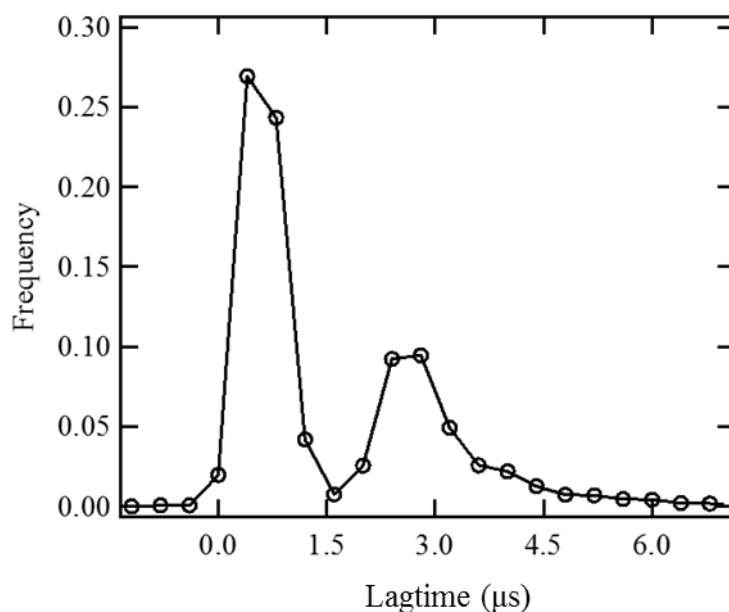
Fig. R4. (Figure S1 in the revised manuscript) The distribution of lag-time in our SP2 measurement.

(7) Fig. 4 and Discussion: The authors assume that BC is the only component of the particles when making their fractal dimension determination. This is an assumption that must be demonstrated in some way. What if, for example, there were a 10 nm thick "coating" on the "externally mixed" BC particles? This might still have a small

lag time. But, depending on the particle size, the mass contribution could be substantial (e.g. for a 100 nm BC core, a 10 nm coating corresponds to nearly 40% of the mass, assuming equal densities and spheres.) How do the authors know that the only component contributing substantially to the particle mass is BC for these particles with small lag times? What sort of uncertainty is contributed by their assumption.

Response: This is a very good point. As the reviewer pointing out, a thin coating on the "externally mixed" BC may cause a large bias in the calculated effective density since particle mass is proportional to D_p^3. However, the effective density was only used to calculate the mobility diameter of externally-mixed BC particles from BC mass measured with SP2. The calculated mobility diameter of BC is with lower bias because diameter is proportional to ρ^{-3}. Taken a 200 nm particle as an example (the smallest size that we selected), assuming a maximum 20 nm thin coating (e.g., as in Subramanian et al., 2010), the bias of the mobility diameter of externally-mixed BC particles would be ~20%.

We will add a caveat in the related discussion and point out the possible error/uncertainties due to the possible thin coating on the externally mixed BC.

(8) P6/L19: The authors state: "For externally-mixed BC particles, a diameter is hard to define due to their irregular morphology." This is not correct. A volume-equivalent or mass-equivalent diameter can be easily defined if the BC mass is measured and it is assumed that the particle is 100% BC (which the authors do here).

Response: Thanks. Here we meant to say "geometric diameter". The sentence has been revised, as "For externally-mixed BC particles, a geometric diameter is hard to define due to their irregular morphology".

(9) I find Fig. 5 unclear. For the mobility distributions (dN/dlogDp vs Dpm), is this from the measurements with the 2nd DMA? This is not stated. If so, why are the peaks

so broad? The size distributions presented suggest that the authors were operating the first DMA with a very low resolution. Is that the case? If so, that would meant that the authors passed through particles with a broad distribution of actual mobility diameters.

Response: Thanks. Fig 5 (in the manuscript) shows the volume-equivalent and mobility diameter distribution of externally mixed BC from SP2 measurements, not from the DMA2. The volume-equivalent diameter distributions were calculated from BC mass and BC material density (1.8 g/cm^3), while the mobility diameter distributions were calculated from BC mass and BC effective density shown in Fig. 4. To make it clear, we revised the caption of Figure 5 as "The volume equivalent diameter (D_{ve}) and mobility diameter (D_m) distribution from SP2 measurement for size-selected externally-mixed BC at (A) 200 nm, (B) 250 nm (B), (C) 300 nm and (D) 350 nm. In SP2 calculation, the D_{ve} of a single BC particle was calculated from BC mass and BC material density (1.8 g cm^{-3}), while the D_m of a single BC particle was calculated from BC mass and the predefined effective density shown in Fig. 4."
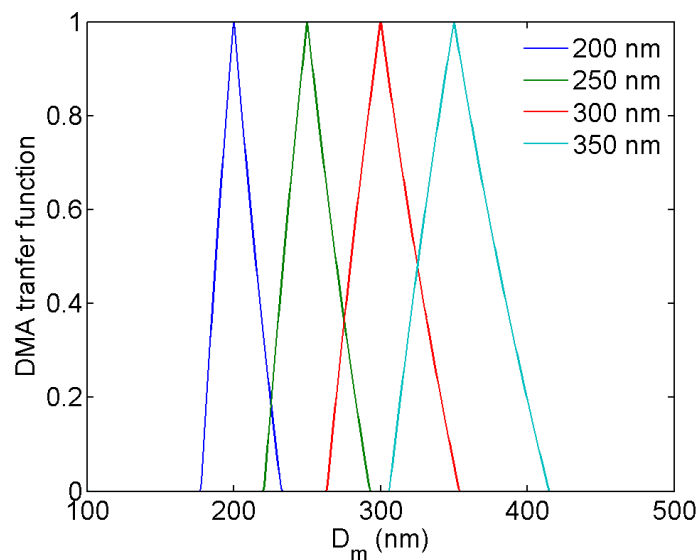
Fig. R5. The theoretical DMA transfer functions at an aerosol to sheath flow ratio of 1:5.

We were not operating the DMA1 with a low resolution. The aerosol to sheath flow ratio of the DMA1 is 1:5. Figure R5 shows the theoretical DMA transfer

functions at this flow ratio. They are much narrower than the mobility distributions shown in Fig. 5 (red lines). The broadening effect caused by DMA transfer function is therefore limited. The broadening of the mobility distributions after the DMA1 is due to the use of a fixed effective density for externally-mixed BC particles when calculating their mobility diameter. Mobility diameter of particles with a certain mass/volume strongly depends on their morphology (quantified as dynamic shape factor). Since externally mixed BC particles are fractal-like agglomerates with varies shape factors (Zhang et al., 2008; Park et al., 2003; Pagels et al., 2009), particles output by the DMA with same or similar mobility may have a large range of mass, meaning also a large range of effective density. However, a fixed effective density was used for deriving the mobility diameters, which caused the broadening effect. We also note here that in each distribution in Fig. 5, the second smaller peak on the right side is due to the double charged particles.

(10) P7, L3: The authors' statements regarding the density of the BC are wrong. The material density is 1.8 g/cm³ (not 1.8 g/m³, as stated). The conversion of the measured mass to a diameter requires specification of what diameter one is considering. One should absolutely use the material density if converting mass to a volume-equivalent diameter. To use a lower effective density is not correct. But, if the authors are aiming to estimate a mobility diameter from the mass, then the use of an effective density is appropriate. But, it is entirely unnecessary here since the argument is circular: the effective density is determined by comparing the selected mobility diameter with the observed volume equivalent diameter. So, conversion of the mass back to a mobility diameter is just a statement of the obvious.

Response: Thanks for the comment. We apologize for the typo, and we have changed the "1.8 g m^{-3}" into "1.8 g cm^{-3}".

We agree with the reviewer that the conversion of the measured mass to a diameter requires specification of what diameter one is considering. The reasons of

showing the mobility diameter distribution are to have a direct comparison with the volume-equivalent diameter.

Following the review's suggestion, we have move Fig. 5 to supplement (Fig. S2) and also made following changes in the manuscript: "Figure 4 shows an effective density of 0.25-0.45 g cm^{-3} for externally-mixed BC particles at 200-350 nm, significantly lower than BC material density of 1.8 g cm^{-3} (Metcalf et al., 2012; Schwarz et al., 2008; Subramanian et al., 2010). The large discrepancy between the effective density and material density of BC indicated that the externally-mixed BC particles measured at Xianghe site was not a void-free sphere, which resulted in significantly differences between volume equivalent diameter (D_{ve}) and the mobility diameter (D_{m}) from SP2 measurement (Figure S2). In this study, we used mobility diameter of externally-mixed BC particles in SP2 measurement to compare with VTDMA measurement."

(11) P7,L9: A tandem DMA is also able to "separate aerosol particles with different charges" if the particle stream is reneutralized. The DMA + SP2 is not unique in this regard.

Response: Thanks to the reviewer to point this out. We do not intent to claim that our approach is the only solution. To clarify it we modified our statement as "Our setup (combination of DMA with SP2) can be used as one method to separate aerosol particles with different charges, similar to the series set up of tandem DMAs with re-neutralizer (Wiedensohler and Fissan, 1991)."

(12) Fig. 6b: I find this to be unclear. Why are there so many points on the graph? There is a fixed ratio between the number of singly and doubly charged particles for each mobility diameter. Thus, there should be one point per size, as is indicated by the text on P7.

Response: Thanks. The different points in Fig. 6B represent samples observed at different days, while the distributions shown in Fig. 6A are the campaign averages. Due to variation of particle number size distribution on different days, the ratio between the number concentrations of singly and doubly charged particles with same mobility is not fixed, resulting in different $R_{single-to-double}$ in Fig. 6B.

To make this point clear, we added "The size distributions in Fig. 6A represents the campaign averages; the different points in the Fig. 6B represents samples observed at different days. Due to variation of particle number size distribution at different days, the ratio between the number concentrations of singly and doubly charged particles with same mobility is not fixed, resulting in different $R_{single-to-double}$" in the caption of Figure 6.

(13) P7/L29: Again, the authors refer to the accuracy of their size determination. But, they have forced agreement. Thus, this is simply a statement that the authors have calibrated their instrument.

Response: Thanks. The main purpose of displaying Fig. 6B is to show that in our experiment SP2 can well distinguish the singly and doubly charged particles. To make this point clear, we have removed "Our results further revealed that the accurate particle size was derived by our method (discussed in Sect. 3.3.1 and Sect. 3.3.2) based on SP2 measurement." in the revised manuscript, and added "which demonstrated that SP2 measurement can distinguish between singly and doubly charged particles. Our results further indicated the potential of optical sizing instruments (e.g., SP2) in determining the bipolar charge distribution of aerosol particles."

(14) Fig. 7: The authors show the SP2 distribution as a sum over different particle types. However, this does not take into account the important issue that the SP2 instrument detection limit is different for scattering and incandescence. The SP2

cannot measure scattering by particles below some size. But this is not the same size below which it cannot measure incandescence. Ultimately, one cannot simply add up the size distributions from the different types of particles from the SP2 without accounting for such effects as it can give a misleading picture.

Response: The SP2 data used in Fig. 7 is based on only incandescence measurements and the different instrument detection limit is not an issue here.

To clarify it, in the caption of Fig. 7, we added "For SP2 data, mobility size of BC component was derived from their mass (determined by SP2 incandescence) and the effective densities (1.2 g cm^{-3} for BC cores of internally-mixed BC particles and 0.25-0.45 g cm^{-3} for BC component of externally-mixed BC particles)."

(15) Fig. 7 and Fig. S2: The authors need to refer to their diameters using some sort

of specific terminology. They are not "rBC diameters." They are, perhaps "mobilityequivalent diameters". The authors must be precise in their terminology. As it is, the lack of precision makes the concepts presented difficult to follow.

Response: Thanks for the suggestion. We have changed "rBC size" into "mobility diameter of BC for BC-containing particles".

(16) P8,L15: It is entirely unclear in what way specifically the "VTDMA measurement had a large uncertainty." What is meant by "uncertainty" here? The VTDMA measurement is what it is. Also, the authors have not demonstrated an ability to measure what are predominately mostly scattering particles below 200 nm: their entire validation exercise used particles with mobility diameters >= 200 nm. It is not surprising that the SP2 does not measure as many purely scattering particles at smaller sizes compared to the VTDMA as it is not designed to do so. What the authors need to show is an efficiency curve, similar to that shown for BC in Fig. S1, but for scattering-only particles. Below what size does the detection efficiency fall off for scattering only particles? Also, it is unclear what the authors mean by a "significant different in BC mixing state" Between the measurements. Different in what way?

What is being determined?

Response: Thanks to the reviewer for raising this concern. VTDMA was designed to measure the refractory residues at certain temperatures. In previous VTDMA-based studies, refractory residues larger than 50 nm at 300 ℃ were usually considered as BC (Philippin et al., 2004; Wehner et al., 2009; and Cheng et al., 2009). In Fig. 7, the discrepancy between the number size distributions of refractory residues and BC cores for diameter larger than 70 nm indicates that at Xianghe site a large fraction of the refractory residuals at 300 ℃ are not BC, suggesting that the assumption made in previous VTDMA studies that most of refractory residuals at 300 ℃ were BC may need to be reconsidered.

To the second question, since we discussed only the distribution of BC cores determined by incandescence signal in SP2. The detection limit of scattering signal did not play a role here. Still, we provide the detection efficiency curve of pure scattering particles for our SP2 here in Figure R6.

To the last question, SP2 gives the mixing state of BC, while VTDMA gives the mixing state of refractory material. They are comparable only if assuming the refractory material at 300 ℃ is BC. But as discussed above, this seems not the case in our study.

$$\eta=1.10-4.20\exp(-0.0164D_p)$$
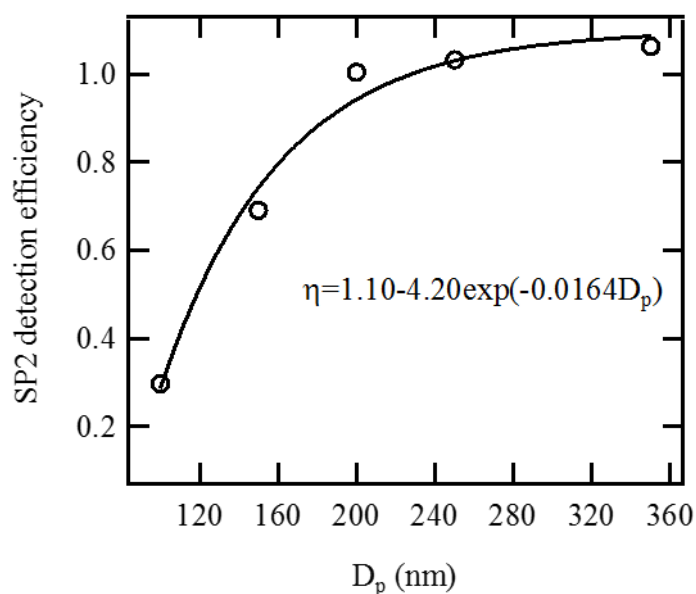
Fig. R6. The SP2 detection efficiencies (η) for non-BC particles at different size (100-350 nm).

We agree with the reviewer that the statement "VTDMA measurement had a large uncertainty" may be misleading here. We have clarified it by rewriting P8/L8-25 as: "Figure 7 shows the mobility size distribution of BC components measured by SP2 and the refractory residues at 300 ℃ measured by VTDMA. The SP2 measurement shows two peaks, one at around the prescribed size (200, 250, 300 and 350 nm selected by DMA1) and another one at a smaller size, representing the externally-mixed BC and internally-mixed BC particles, respectively. For VTDMA measurement, the number size distribution of low-volatile residues at 300 ℃ also shows a peak at the prescribed size (selected by the DMA1), and other peaks at smaller sizes, which is similar to the previous measurements in Beijing (Cheng et al., 2012). Above the detection limit of SP2 incandescence (larger than 70 nm BC particles), the number concentration of BC particles measured by SP2 accounted for only 16-35% of residual particles measured by VTDMA. This large discrepancy indicated a large fraction of non-BC low-volatile components which could not completely volatile at 300 ℃ (e.g. refractory OM, mineral dust, trace metals and sea salt) (Cheng et al., 2009; Ehn et al., 2014; Kalberer et al., 2004) exists in the aerosol particles at Xianghe site. Furthermore, we found that most of the non-shrinking refractory residues (~78-91%) (the 1st peak of the DMA2) are detected as BC particles by SP2, while there are about 80-90% of the residues in the 2nd peak of the DMA2 (shrank particles) are not BC, as they did not show incandescence signal in SP2. In previous VTDMA studies, it has often been assumed that the refractory residual materials at 300 ℃ were BC components (Philippin et al., 2004; Wehner et al., 2009; and Cheng et al., 2009). But, this assumption may not hold at the sub-urban site of Beijing (Xianghe), and may cause a significantly overestimation of the number of internally mixed BC particles and lead to large uncertainties in BC radiative forcing estimations in the North China Plain."
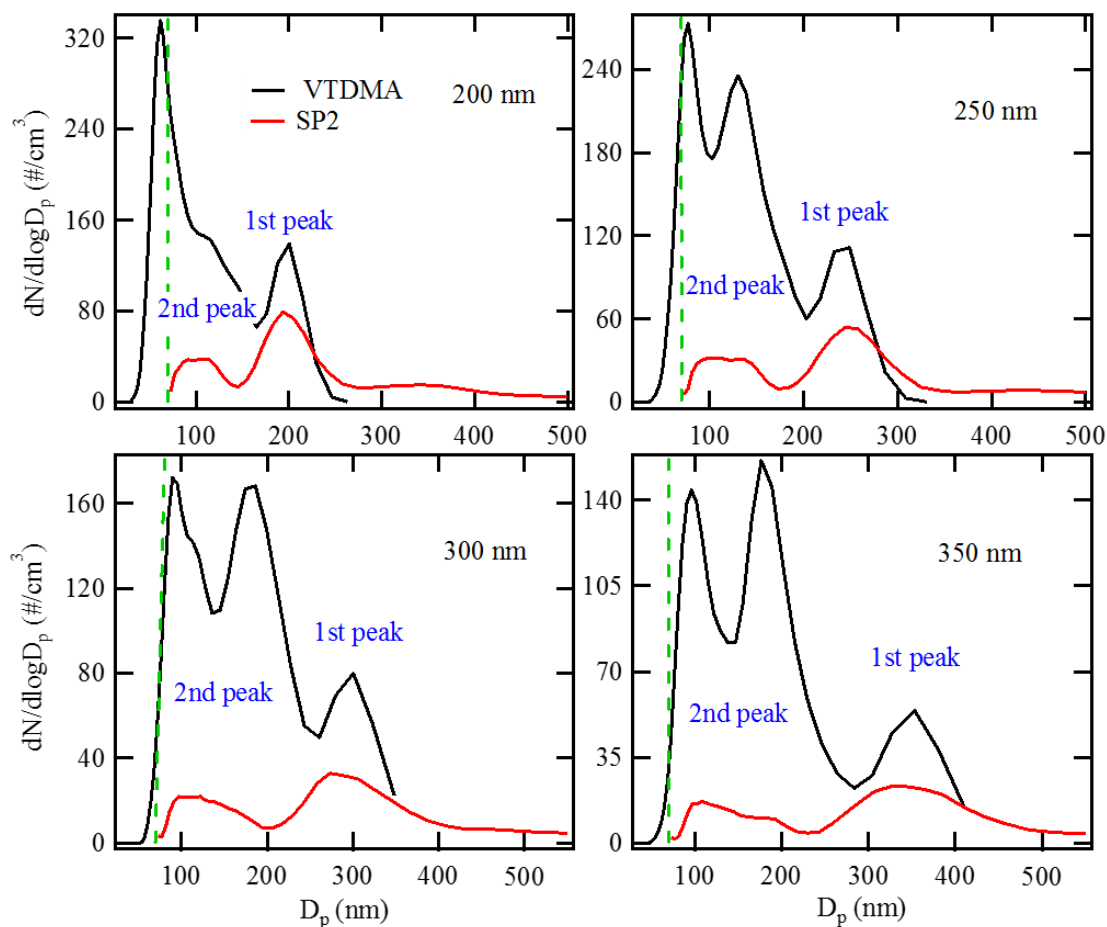
Fig. R7. (Figure 7 in the revised manuscript) Mobility size distributions of BC for BC-containing particles measured by SP2 (red lines) and that of residual materials from our VTDMA measurement at 300 ℃ (black lines). The green dash line reflects the lower limit of SP2 incandescence detection (~70 nm). Before the measurements were taken with SP2 and VTDMA at 300 ℃, the initial particle sizes selected by DMA1 were 200, 250, 300 and 350 nm. For SP2 data, mobility size of BC component was derived from their mass (determined by SP2 incandescence) and the effective densities (1.2 g cm^{-3} for BC cores of internally-mixed BC particles and 0.25-0.45 g cm^{-3} for BC component of externally-mixed BC particles). Note that the SP2 detection efficiency and experimentally determined effective density have been considered in the calculation of the rBC size distribution (Fig. S4).

(17) P8/L14-25: I find this paragraph very difficult to understand. The SP2 cannot

measure small particles. I do not see how comparing the SP2 to the VTDMA in this particular way is addressing limitations of the VTDMA.

Response: Thanks to the reviewer to raise this concern. Sorry for the misleading and we are not aiming to addressing the limitation of VTDMA. Here, we only compare the number size distribution of refractory residues measured by the DMA2 of VTDMA and the BC particles detected by SP2 above its incandescence detection limit (>70 nm BC particles). The number size distribution of BC cores from SP2 measurement (red lines in Fig. 7) is corrected for SP2 incandesce particle-counting efficiency according to calibration curve (Fig. R8 in response). Therefore, the detection limit of scattering signal is not an issue here.
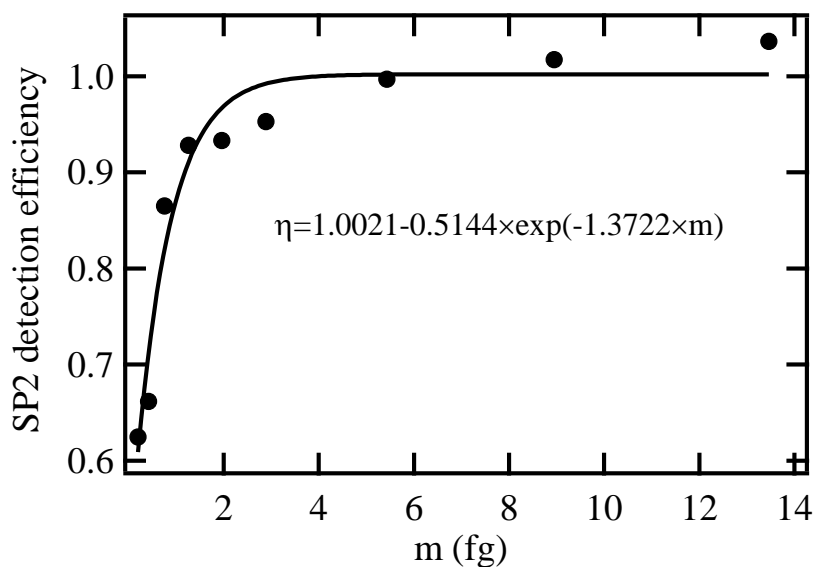
Fig. R8 (Figure S4 in the revised manuscript). The SP2 detection efficiencies (η) in each BC mass-bin.

The last two paragraphs in Sect. 3.2 have been rewritten according to the two comments above (see the above response).

(18) Fig. 7 vs. Fig. 8: Considering the authors' own measurements, there is an inconsistency between these two figures. The SP2 size distributions shown in Fig. 7 suggest that the distribution is dominated by "externally-mixed BC" particles. But,

Fig. 8 clearly indicates that the number is dominated by "non-BC" particles. Fig. 8 is thus more consistent with the VTDMA measurements shown in Fig. 7, which shows a substantial fraction of what might be considered "non-BC" particles (i.e. the particles that shrank a lot). Yet, the authors just spent a section arguing that the SP2 does a better job than the VTDMA. These discussions must be aligned and reconciled..

Response: Thanks to the reviewer. There might be some misunderstanding. In Fig. 7, we discussed about BC-containing particles (internally-mixed BC and externally-mixed BC particles). But, Fig. 8A shows the number fractions of all particles (i.e., non-BC, internally-mixed BC and externally-mixed BC particles).

To make it clear, we revised the caption of Figure 8 as "(A) The number and (B) mass composition of ambient particle samples (non-BC, externally-mixed BC and internally-mixed BC) with different mobility diameters (200, 250, 300 and 350 nm) selected by DMA1.**"**

(19) P9,L6: It is unclear how a small BC fraction necessarily indicates "long range transport." This must be justified. Yes, it suggests that there is secondary processing (most likely), but why "long range transport" specifically? The authors seem to take this as a given. Why not local photochemical or nocturnal processing?

Response: Thanks for the comment. We agree with the reviewer that the aging of BC particles may not need to experience the long-range transport. BC is primary aerosol component emitted during combustion process (biomass and fossil fuel burning). BC aging degree (i.e., coating thickness and D_p/D_c ratio) in the atmosphere strongly depends on secondary processing (Metcalf et al., 2013). The more secondary aerosols (i.e., non-BC species such as SOA, sulfate and nitrate) formed in the atmosphere the higher BC aging degree and thicker coating. BC aging process may occur locally or during regional transport. In this study, we cannot distinguish between them.

We have changed "long range transport" into "secondary process" and in manuscript it reads as "revealed that the aerosol particles sampled at our site was likely

underwent a strongly secondary process."

(20) P9/L11: The authors state here that the fraction of internally-mixed particles at 200-300 nm was 38-51%. But, above, they say that these particles are only 7-10%, including externally-mixed particles. Clearly there is a discrepancy. Fig. 8 and Fig. 9 are similarly inconsistent. Perhaps they are talking about only the BC-containing particles. But this is unclear.

Response: Thanks. In Fig. 8, we talked about all particles, including non-BC, internally-mixed BC and externally-mixed BC particles. In Fig. 9, we talked about only the BC-containing particles.

To make it clear, we have changed the "the fraction of internally-mixed particles" in P9/L11 into "the fraction of internally-mixed BC-containing particles".

(21) P9/L13: How do the authors know that the peak is from both photochemical formation and regional transport? How is the influence of regional transport identified? Why not just local production?

Response: Thanks. As responded to comment (19), we have changed "The peak around noontime can be attributed to secondary photochemical formation and regional transport" into "The peak around noontime can be attributed to physico-chemical aging (Cheng et al., 2012)."

(22) P9/L16: The authors compare their current results to those of Cheng et al. for Beijing. They should note that Cheng et al. also made measurements in Beijing.

Response: Thanks for the suggestion. The sentence has been revised as "which was consistent with the findings of Cheng et al. (2012) at another site in Beijing (~60 km from Xianghe site)".

(23) Fig. 10: Much more meaningful would be a histogram of the Dp/Dc values. The justification for binning as was done here is not clear.

Response: Following reviewer's suggestion, we have changed the Fig. 10 into a histogram. As shown below (Figure R9 and R10 in response):
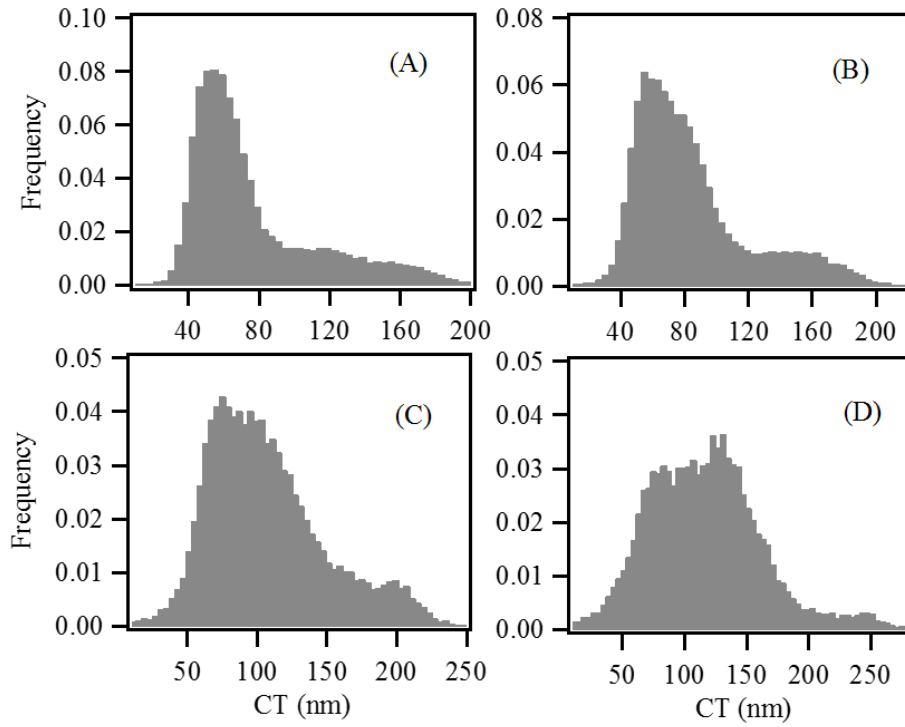
Figure. R9. (Figure 10 in the revised manuscript) The frequency distribution of coating thickness (CT) for internally-mixed BC with different mobility diameters ((A) 200, (B) 250, (C) 300 and (D) 350 nm) selected by DMA1.
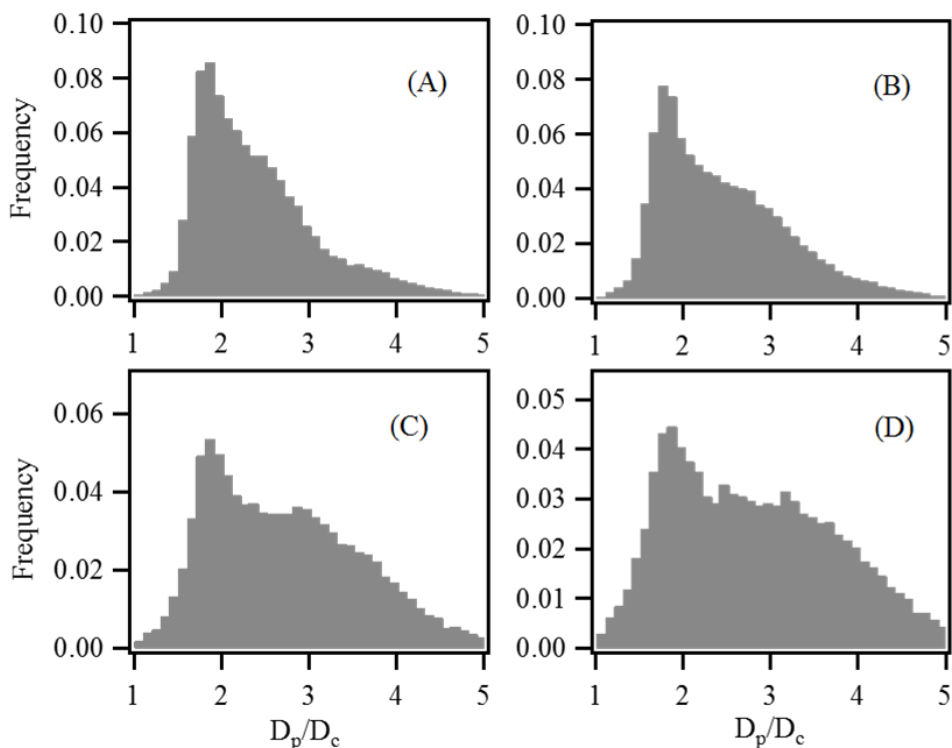
Figure. R10 (Figure. S5 in the revised manuscript). The frequency distribution of D_p/D_c ratio for internally-mixed BC with different mobility diameters ((A) 200, (B) 250, (C) 300 and (D) 350 nm) selected by DMA1.

Correspondingly, we also revised the discussion on Figure 10: "Figure 10 shows the frequency distributions of *CT* of internally-mixed BC particles at 200-350 nm. The observed internally-mixed BC particles are dominated by particles with *CT* of 40-200 nm. The average *CT* of internally-mixed BC particles at 200, 250, 300 and 350 nm were respectively 74, 80, 100 and108 nm, accompanying with average D_p/D_c ratio of 2.3, 2.4, 2.6 and2.7 (Fig. S5)."

(24) P9/L20: It is not at all surprising that the "internally-mixed" particles have thick coatings. This is by definition, as the authors have discriminated by the difference in lag times and thus we would fully expect that the particles should have large Dp/Dc ratios. If they did not, they would not have been identified as "internally mixed" in

the first place. What is the relationship between lag time and Dp/Dc for this study? How are the authors skewing their analysis by deciding on a particular lag time cutoff.

Response: Thanks to the reviewer. The lag-time method is commonly used in previous SP2 studies (e.g., Schwarz et al., 2006; Sedlacek et al., 2012; Subramanian et al., 2010). We know it might not be the perfect way, but currently it is the only way to get the mobility diameter distribution of both externally mixed BC and BC cores in internally mixed particles from SP2 measurement. The reason is that we cannot retrieve the optical diameters of externally mixed BC with Mie model is because they may have irregular shapes (Fig. 4 in the manuscript). This is also a limitation of SP2 technique. There is no simple relation between lag time and Dp/Dc, since the lag time also depends on the location of BC core in particles.

By "thick coating" and "strongly enhanced absorption", we didn't mean to compare with un-coated (externally mixed) BC, but to compare with results at other less polluted locations. The bimodal distribution of lag-time is commonly observed, e.g., in Long Island site (Sedlacek et al., 2012), Mexico site (Subramanian et al., 2010), where the coating thickness (~30-60 nm) of internally-mixed BC is thinner than that of our study.

To make it clear, we added "Considering irregular shape of externally-mixed BC particles, we only calculated the coating thickness of internally-mixed BC particles using Mie mode in this study. The observed internally-mixed BC aerosols in NCP are dominated by particles with *CT* of 40-200 nm. On average, the *CT* of internally-mixed BC particles at 200-350 nm were 74-108 nm, which significantly larger than that at other less polluted locations (Sedlacek et al., 2012; Subramanian et al., 2010)." in the manuscript.

(25) P9/L22: The authors should comment further on the observation that Dp/Dc increases as Dp increases. (They might even make a plot…). Why do they think this is the case? What physical insights can be discerned?

Response: As shown in Fig. R12, core diameters of BC-containing particles have a

narrow distribution with mode centers located at 100-150 nm, since BC is primary aerosol component. Therefore, larger particles usually have also a thicker coating and larger D_p/D_c (Fig. R11), as a consequence of condensation and coagulation, which happen mostly between BC and non-BC species.

To make it clear, we revised the sentence as "Both the average CT and D_p/D_c ratio at 200-350 nm increased as the particle size increases (Fig. S6), which can be attributed to the condensation and coagulation between BC and non-BC species during the atmospheric process. Fig. S7 shows that core diameters of BC-containing particles have a narrow distribution with mode centers located at 100-150 nm, since BC is primary aerosol component and can not be produced secondarily. Therefore, larger particles usually have also a thicker coating and larger D_p/D_c."
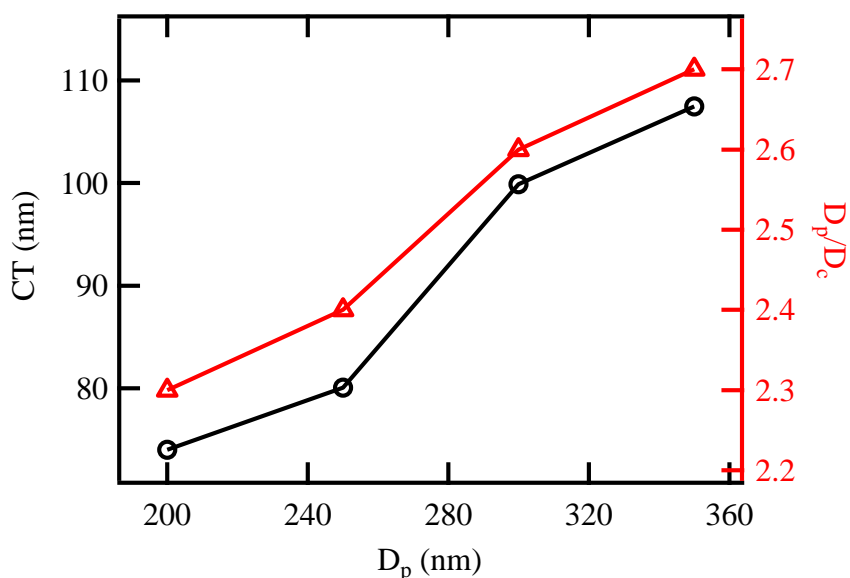
Fig. R11. (Figure S6 in the revised manuscript). The average CT and D_p/D_c ratio at different size (200-350 nm).
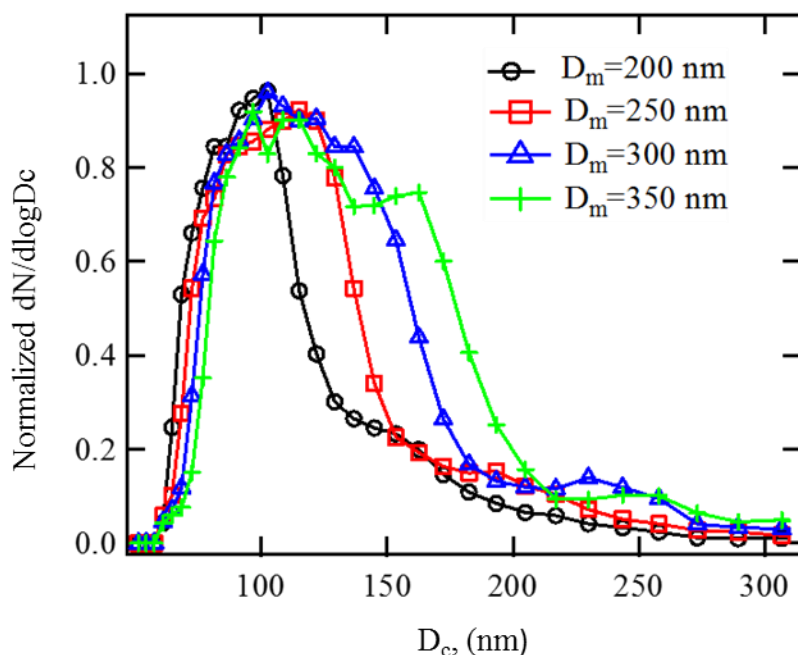
Fig. R12. (Figure S7 in the revised manuscript). The number size distribution of BC cores for internally-mixed BC.

(26) P9/L22: The authors again point to long range transport. Why is local photochemical production of coatings not possible, especially given that there is clearly a local source of BC?

Response: Thanks for the comment. We agree that this statement is inappropriate. We have changed "long range transport" into "secondary process". See response to (19).

(27) P9/L27: The authors cite Zhang et al., (2016b) to support their statements regarding potential for absorption enhancement. But, (i) Zhang et al simply provide calculations that say that when BC particles are coated absorption can be enhanced, which has been known for a long time since before Zhang and (ii) the Zhang results are simply calculations, and the actual magnitude of absorption enhancements in the atmosphere remains unresolved. The authors should provide a fuller discussion and not simply self-cite.

Response: Thanks for the comment. We have deleted the sentence and added the following discussion in the manuscript, as shown below:

"The thick coatings of internally-mixed BC particles indicated that their light absorption might be enhanced by lensing effects (Fuller et al., 1999; Lack and Cappa 2010; Liu et al. 2015; Moffet et al., 2009). However, the actual magnitude of absorption enhancements of BC aerosol in the atmosphere remains unresolved due to complex morphology and inhomogeneity of ambient BC-containing particles (Adachi et al. 2013; Cappa et al. 2012; Fuller et al. 1999; Liu et al. 2015; Liu et al. 2017). The agreement between optical size and mobility size shown in Fig. 3 indicated that the internally-mixed BC particles observed in our study were nearly spherical due to strong aging process. The absorption enhancement of spherical BC particle strongly depends on the coating amount on BC surface (Fuller et al. 1999; Lack and Cappa 2010; Liu et al. 2017), indicating that the light absorption of internally-mixed BC particles in the NCP could be significantly enhance due to thick coatings."

(28) Fig. 11: This figure is fundamentally misleading. The SP2 cannot measure the size of particles via the optical method if they are too small. The lower-limit size differs for BC measurement vs. for size measurement. Thus, there is an intrinsic bias in the method that makes it appear as if the coating thicknesses of small BC particles are larger, on average, than they might be. Consider a 100 nm core. If the smallest optical diameter that can be measured is 150 nm, then the thinnest coating is 25 nm. There is no information about the concentration of 100 nm cores with CT < 25 nm. It may be that the decrease in coating thickness with core size, shown in Fig. 11, is valid. But, the authors must demonstrate that their measurements are not biased by differences in the lower-limit size for BC vs. for optics.

Response: Thanks for the comment. The effect pointed out by the reviewer only exists when measuring poly-dispersed aerosol with SP2 (without a DMA upstream) due to a fraction of particles with size lower than SP2 detection limit. But in our study, we do not have such a problem since what we measured is mono-dispersed aerosol particles (pre-selected by the DMA1) with diameters higher than the scattering detect limit of SP2 (200, 250, 300, 350 nm vs. ~200 nm).

(29) Fig. 11: The authors say that their curves follow "diffusion-controlled growth." But, looked at another way there is absolutely no reason to think that they would obtain any other result, given their method. They size select at a given size. And they measure a core size. By definition, Dselected = Dcore + 2*CT. Thus, there is a definite relationship between their coating thickness and Dcore. Further, the curves shown generally follow this curve. For a 100 nm core, the "coating thickness" for a 200, 250, 300 and 350 nm selected size is 50, 75, 100 and 125 nm. These are nearly identical to what the authors obtain. In other words, their graphs show exactly what is expected based on simple algebra, with no need to invoke "diffusion-controlled growth." Or, put another way, the results do not provide any information on the growth mechanism nor do they demonstrate that coating thicknesses decrease with core diameter. The entire discussion regarding Fig. 10 needs to be either removed or substantially revised. And if revised, needs to move beyond the simple algebraic expectation to provide some physical insight.

Response: Thanks for the comment. We agree with the reviewer that we can not conclude "diffusion-controlled growth" from Fig. 11 (Fig. R13 in response). We have deleted the statement in the manuscript.

However, Fig. 11 (Fig. R13 in response) provides additional information on the relation between coating thicknesses and core size. For a certain core, the coating thickness in Fig. 11 shows a wide range rather than a value of $CT=(D_{selected}-D_{core})/2$, because the size of the particles selected by DMA still exhibited a distribution. Moreover, Figure 11 also shows the modes of coating thickness for the doubly and triply charged particles (black and gray dashed lines in Fig. R13).
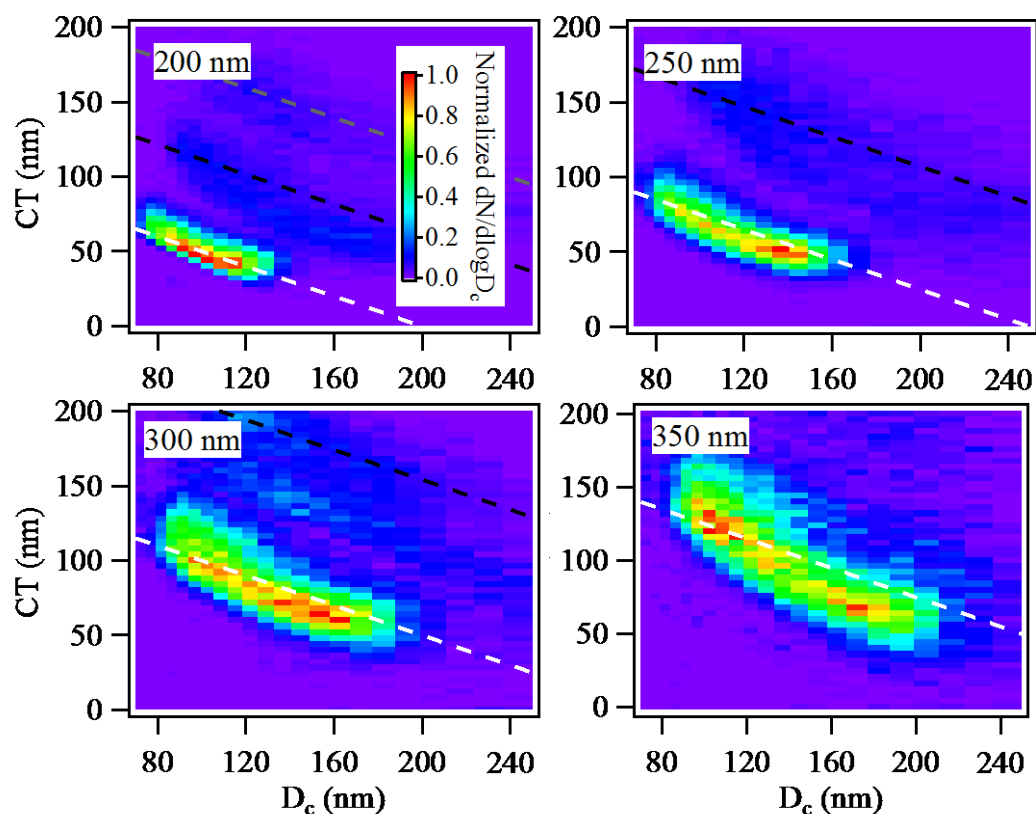
Fig. R13 (Figure S8 in the revised manuscript). Coating thickness (CT) of internally-mixed BC particles at 200-350 nm (selected by DMA1) as a function of rBC core size (Dc). The dash line is $CT=(D_{selected}-D_c)/2$, i.e., the theoretic CT; the white, black and grey colors reflect the singly, doubly and triply charged particles.

Since Fig. 11 gives some information of the influence of DMA transfer function and multiple charged particles on the distribution of CT, we decided to move it to Supplement (Fig. S8). We have modified Fig. 11. The discussion on Fig. 11 have be revised in the manuscript "Figure S8 shows the coating thickness of internally-mixed BC particles as a function of rBC core size (D_c). For a certain core, the coating thickness in Fig. S8 shows a wide range rather than a value of $CT=(D_{selected}-D_c)/2$, because the size of the particles selected by DMA still exhibited a distribution. For singly charged particles (white dashed lines in Fig. S8) at 200-350 nm, the D_c and CT showed a wide mode, which were in the range of ~80-200 nm and ~50-150 nm, respectively. Moreover, Figure S8 also shows the modes of coating thickness for the doubly and triply charged particles (black and gray dashed lines in Fig. S8). The wide

range of D_c and CT revealed that the internally-mixed BC particles at our site consisted of a mixture of BC from various sources of the North China Plain. The more coatings on BC the longer secondary process BC-containing particles undergoing."

References:

Adachi, K., and Buseck, P. R.: Changes of ns-soot mixing states and shapes in an urban area during CalNex, *J. Geophys. Res.: Atmos.*, 118, 3723-3730, 2013.

Cappa, C. D., Onasch, T. B., Massoli, P., Worsnop, D. R., Bates, T. S., Cross, E. S., Davidovits, P., Hakala, J., Hayden, K. L., Jobson, B. T., Kolesar, K. R., Lack, D. A., Lerner, B. M., Li, S. M., Mellon, D., Nuaaman, I., Olfert, J. S., Petaja, T., Quinn, P. K., Song, C., Subramanian, R., Williams, E. J., and Zaveri, R. A.: Radiative Absorption Enhancements Due to the Mixing State of Atmospheric Black Carbon, *Science*, 337 (6098), 1078-1081, 2012.

Cheng, Y., Berghof, M., Garland, R. M., Wiedensohler, A., Wehner, B., Müller, T., Su, H., Zhang, Y., Achert, P., Nowak, A., Pöschl, U., Zhu, T., Hu, M., and Zeng, L.: Influence of soot mixing state on aerosol light absorption and single scattering albedo during air mass aging at a polluted regional site in northeastern China, *J. Geophys. Res.*, 114, (D10), D010883, 2009.

Cheng, Y. F., Su, H., Rose, D., Gunthe, S. S., Berghof, M., Wehner, B., Achtert, P., Nowak, A., Takegawa, N., Kondo, Y., Shiraiwa, M., Gong, Y. G., Shao, M., Hu, M., Zhu, T., Zhang, Y. H., Carmichael, G. R., Wiedensohler, A., Andreae, M. O., and Pöschl, U.: Size-resolved measurement of the mixing state of soot in the megacity Beijing, China: diurnal cycle, aging and parameterization, *Atmos. Chem. Phys.*, 12, 4477-4491, 2012.

Ehn, M., Thornton, J. A., Kleist, E., Sipila, M., Junninen, H., Pullinen, I., Springer, M., Rubach, F., Tillmann, R., Lee, B., Lopez-Hilfiker, F., Andres, S., Acir, I.-H., Rissanen, M., Jokinen, T., Schobesberger, S., Kangasluoma, J., Kontkanen, J., Nieminen, T., Kurten, T., Nielsen, L. B., Jorgensen, S., Kjaergaard, H. G., Canagaratna, M., Maso, M. D., Berndt, T., Petaja, T., Wahner, A., Kerminen, V.-M., Kulmala, M., Worsnop, D. R., Wildt, J., and Mentel, T. F.: A large source of low-volatility secondary organic aerosol, *Nature*, 506, 476-479, 2014.

Fuller, K. A., Malm, W. C., and Kreidenweis, S. M.: Effects of mixing on extinction by carbonaceous particles, *J. Geophys. Res.-Atmos.*, 104, 15941-15954, 1999.

Gao, R. S., Schwarz, J. P., Kelly, K. K., Fahey, D. W., Watts, L. A., Thompson, T. L., Spackman, J. R., Slowik, J. G., Cross, E. S., Han, J. H., Davidovits, P., Onasch, T. B., and Worsnop, D. R.: A Novel Method for Estimating Light-Scattering Properties of Soot Aerosols Using a Modified Single-Particle Soot Photometer, *Aerosol Sci. Technol.*, 41, 125-135, 2007.

Hänel, G.: The real part of the mean complex refractive index and the mean density of samples of atmospheric aerosol particles, *Tellus*, 20, 371-379, 1968.

Kalberer, M., Paulsen, D., Sax, M., Steinbacher, M., Dommen, J., Prevot, A. S. H., Fisseha, R., Weingartner, E., Frankevich, V., Zenobi, R., and Baltensperger, U.: Identification of Polymers as Major Components of Atmospheric Organic Aerosols, *Science*, 303, 1659-1662, 2004.

Lack, D. A. and Cappa, C. D.: Impact of brown and clear carbon on light absorption enhancement, single scatter albedo and absorption wavelength dependence of black carbon, *Atmos. Chem. Phys.*, 10, 4207–4220, 2010.

Liu, D., Whitehead, J., Alfarra, M. R., Reyes-Villegas, E., Spracklen, D. V., Reddington, C. L., Kong, S., Williams, P. I., Ting, Y.-C., Haslett, S., Taylor, J. W., Flynn, M. J., Morgan, W. T., McFiggans, G., Coe, H., and Allan, J. D.: Black-carbon absorption enhancement in the atmosphere determined by particle mixing state, *Nature Geosci*, 10, 184-188, 2017.

Liu, S., Aiken, A. C., Gorkowski, K., Dubey, M. K., Cappa, C. D., Williams, L. R., Herndon, S. C., Massoli, P., Fortner, E. C., Chhabra, P. S., Brooks, W. A., Onasch, T. B., Jayne, J. T., Worsnop, D. R., China, S., Sharma, N., Mazzoleni, C., Xu, L., Ng, N. L., Liu, D., Allan, J. D., Lee, J. D., Fleming, Z. L., Mohr, C., Zotter, P., Szidat, S., and Prévôt, A. S. H.: Enhanced light absorption by mixed source black and brown carbon particles in UK winter, *Nat Commun.*, 6, 8435, 2015.

Marley, N. A., Gaffney, J. S., Baird, J. C., Blazer, C. A., Drayton, P. J., and Frederick, J. E.: An Empirical Method for the Determination of the Complex Refractive Index of Size-Fractionated Atmospheric Aerosols for Radiative Transfer Calculations, *Aerosol Sci. Technol.*, 34, 535-549, 2001.

Metcalf, A. R., Craven, J. S., Ensberg, J. J., Brioude, J., Angevine, W., Sorooshian, A., Duong, H. T., Jonsson, H. H., Flagan, R. C., and Seinfeld, J. H.: Black carbon aerosol over the Los Angeles Basin during CalNex, *J. Geophys. Res.-Atmos.*, 117, 2012.

Moffet, R. C. and Prather, K. A.: In-situ measurements of the mixing state and optical properties of soot with implications for radiative forcing estimates, P. Natl. Acad. Sci. USA, 106, 11872–11877, 2009.

Pagels, J., Khalizov, A. F., McMurry, P. H., and Zhang, R. Y.: Processing of Soot by Controlled Sulphuric Acid and Water Condensation Mass and Mobility Relationship, Aerosol Sci. Technol., 43 (7), 629-640, 2009.

Park, K., Cao, F., Kittelson, D. B., and McMurry, P. H.: Relationship between particle mass and mobility for diesel exhaust particles, Environ. Sci. Technol., 37 (3), 577-583, 2003.

Philippin, S., Wiedensohler , A., and Stratmann, F.: Measurements of non-volatile fractions of pollution aerosols with an eight-tube volatility tandem differential mobility analyzer (VTDMA-8), *Aerosol Sci.*, 35, 185-203, 2004.

Schkolnik, G., Chand, D., Hoffer, A., Andreae, M. O., Erlick, C., Swietlicki, E., and Rudich, Y.: Constraining the density and complex refractive index of elemental and organic carbon in biomass burning aerosol using optical and chemical measurements, *Atmos. Environ.*, 41, 1107-1118, 2007.

Schwarz, J. P., Gao, R. S., Spackman, J. R., Watts, L. A., Thomson, D. S., Fahey, D. W., Ryerson, T. B., Peischl, J., Holloway, J. S., Trainer, M., Frost, G. J., Baynard, T., Lack, D. A., de Gouw, J. A., Warneke, C., and Del Negro, L. A.: Measurement of the mixing state, mass, and optical size of individual black carbon particles in urban and biomass burning emissions, *Geophys. Res. Lett.*, 35, 2008.

Schwarz, J. P., Gao, R. S., Fahey, D. W., Thomson, D. S., Watts, L. A., Wilson, J. C., Reeves, J. M., Darbeheshti, M., Baumgardner, D. G., Kok, G. L., Chung, S. H., Schulz, M., Hendricks, J., Lauer, A., Kärcher, B., Slowik, J. G., Rosenlof, K. H., Thompson, T. L., Langford, A. O., Loewenstein, M., and Aikin, K. C.: Single-Particle Measurements of Midlatitude Black Carbon and Light-Scattering Aerosols from the Boundary Layer to the Lower Stratosphere, *J. Geophys. Res.: Atmos*., 111 (D16), D16207, 2006.

Sedlacek, A. J., Lewis, E. R., Kleinman, L., Xu, J., and Zhang, Q.: Determination of and evidence for non-core-shell structure of particles containing black carbon using the Single-Particle Soot Photometer (SP2), *Geophys. Res. Lett.*., 39 (L06802), L050905, 2012.

Subramanian, R., Kok, G. L., Baumgardner, D., Clarke, A., Shinozuka, Y., Campos, T. L., Heizer, C. G., Stephens, B. B., de Foy, B., Voss, P. B., and Zaveri, R. A.: Black carbon over Mexico: the effect of atmospheric transport on mixing state, mass absorption cross-section, and BC/CO ratios, *Atmos. Chem. Phys*., 10, 219-237, 2010.Wehner, B., Berghof, M., Cheng, Y. F., Achtert, P., Birmili, W., Nowak, A., Wiedensohler, A., Garland, R. M., Pöschl, U., Hu, M., and Zhu, T.: Mixing state of nonvolatile aerosol particle fractions and comparison with light absorption in the polluted Beijing region, *J. Geophys. Res*., 114 (D17): D010923, 2009.

Wiedensohle, A., and Fissan, H. J.: Bipolar Charge Distributions of Aerosol Particles in High-Purity Argon and Nitrogen, *Aerosol Sci. Technol.*, 358-364, 1991.

Zhang, R., Khalizov, A. F., Pagels, J., Zhang, D., Xue, H., and McMurry, P. H.: Variability in morphology, hygroscopicity, and optical properties of soot aerosols during atmospheric processing, Proc. Natl. Acad. Sci. USA., 105 (30), 10291-10296, 2008..